Minimal Rational Interpolation and Its Application in Fast Broadband Simulation

JUN WEI WU AND **TIE JUN CUI**, (Fellow, IEEE)

State Key Laboratory of Millimeter Wave, Southeast University, Nanjing 210096, China

Corresponding author: Tie Jun Cui (tjcui@seu.edu.cn)

ABSTRACT Broad bandwidth simulation in frequency domain benefits from fast frequency sweep, and frequency-domain electromagnetic solvers are usually combined with asymptotic wave evaluation or interpolation techniques. In this work, we introduce the minimal rational interpolation from the perspective of linear algebra and utilize it in fast broadband simulation. An efficient approach is formed by combining adaptive frequency sampling and rational interpolating. Approximate models of the quantities of interests are updated iteratively until the the broadband spectral dynamics are captured. Thanks to the minimal rational interpolation, the approach is fully automatic and does not require pre-estimates of the orders of interpolating functions in each step of the iterations. The obtained functions always have low complexities, hence no further model order reduction is needed. Broadband simulations on admittance of a multi-port interconnects and backward scattering of a cube are given as numerical examples. Results show that the approach can significantly improve the computational efficiency.

INDEX TERMS Broadband simulation, fast frequency sweep, rational interpolation, asymptotic wave evaluation, adaptive frequency sampling.

I. INTRODUCTION

Applications like broadband antenna design, radar cross section (RCS) reduction, high-speed interconnects analysis, and macromodel extraction require spectral responses of electromagnetic (EM) systems over broad bandwidth. Numeric simulation with computational electromagnetic (CEM) solver is an economic and accurate way to get such responses. Frequency-domain solvers are appealing due to their advantages in terms of efficiency and accuracy. However, direct application of frequency-domain solvers for broadband simulation is inefficient since large number of frequencies have to be simulated and much time will be cost. A lot of work has been reported on the topic of efficient broadband simulation with frequency-domain solvers [1]–[19]. Most of these study is in the framework of model based parameter estimation

The associate editor coordinating the review of this manuscript and approving it for publication was Chan Hwang See.

[1]–[3], where physics-based models are applied to describe the variation of system variables over frequency.

Multipath excitation model is utilized to extrapolate currents over frequency in [4], and phase extracted basis is used to analyze the broadband scattering of perfect electrical conductors (PEC) in [5]. Asymptotic wave evaluation (AWE) [6], [20] employs moments matching to generate broadband series expressions, and it has been combined with the method of moments (MOM) and the finite element method (FEM) [7]–[9]. Similar idea is used to solve low-frequency complex problems over a frequency range [8], [10]. However, Taylor series expansion is only valid near the expansion point, and quantitatively predicting how far one can deviate from the expansion point is difficult. Series model contains only zeros (i.e., polynomial model), therefore it is not capable of describing the contributions of poles. From this point of view, AWE has inherent drawback. Zero-pole model (i.e., rational function model) is more natural for representing the variation of system variable over frequency. As a result,

the Padé approximation, which converts polynomials into rational functions, is usually used to expand the valid bandwidth of AWE. In addition, multi-point expansion is also applied to expand the bandwidth. Another drawback of AWE is that it increases the memory and time costs of numeric solvers, as high order derivatives must be calculated and kept in memory and a group of equations have to be solved. In addition, the original CEM codes must be modified in order to implement AWE. For integral equation based methods, the computational cost and the amount of work to modify the codes grow drastically.

As mentioned before, zero-pole model is more suitable for characterizing the variations of system variables over frequency, so a straight forward idea is to use rational interpolating functions directly. To this end, a group of representative frequencies are selected from the desired frequency range, and EM simulations are carried out at these points. Then the simulation results are fitted by rational interpolating functions, which are believed to be accurate over the frequency range. By this way, the original codes remain unchanged. Various methods have been introduced following this idea, and they differ in the methods of finding the degrees and coefficients of the rational functions.

In Cauchy method [11], [12], estimates of the degrees of the numerator and denominator polynomials should be given first, then singular value decomposition (SVD) is performed on a data matrix to find the redundancy in the estimates. If there is no redundancy, the estimates have to be increased until the redundancy appears. Then the polynomial degrees are corrected and the coefficients are solved by the total least squares method. Vector fitting has been used widely since 1999 [13]. It employs pole relocation to generate pole-residue model of given data. Combined with adaptive frequency sampling (AFS) and the partial element equivalent circuit (PEEC) method [21], it can be used for extracting macromodel of interconnects [14]. However, in vector fitting estimate of the degree of rational function is also required. If the degree is underestimated, the fitting results will be inaccurate. In this case, the estimated degree must be increased. Conversely, when the degree is overestimated, the resulting rational function will be unnecessarily complex. Thiele's continued fraction and algorithms of Neville type solve rational interpolation problems recursively [15], [16], [22]. Within each step of recursion, either the degree of numerator or the degree of denominator increases by one. At the end of recursion, the summation of the degrees of numerator and denominator will be $K - 1$, where K is the total number of interpolating data. This leads to rational functions that are more complex than actually needed.

Summarizing the above interpolation-based methods, we see that in Cauchy method and vector fitting, degrees of rational functions must be prescribed first. Cut-and-try process may be performed several times in a single interpolation task. This prevents the two methods from being applied in efficient and fully automatic broadband simulation. In vector fitting, Thiele's continued fraction and algorithms

of Neville type, rational functions are not guaranteed to have low complexities, which are appealing in view of numerical stability and physical realization. Consequently, model order reduction should be carried out as post-processing.

Recently, the minimal rational interpolation (MiniInt) is exploited to model the variations of system variables over frequency [17]–[19], [23], [24]. Given a group of data, it seeks rational interpolating functions with the minimal McMillan degree. The problem was first solved in 1986 [25]. In the work, the underlying degree of rational function is regarded as the number of significant singular values of the Loewner matrix pencil. State space representation of the system is found by projecting data matrices on the singular vectors, and rational interpolation matrix is constructed based on the state space representation. We here call the method the Loewner matrix method. An alternative solution of the minimal rational interpolation problem was proposed in 1990 [26], [27]. In the method, interpolating function with the minimal McMillan degree is found automatically, hence heuristic estimates of the degree of the rational function is not required. This feature facilitates the application of the method in fast broadband simulation. The method was originally introduced in [26], [27] from the perspective of linear system and control theory. To the best of our knowledge, it has remained largely unknown to the EM, RF, and circuit communities. The subjects of this paper are to give an alternative and simple interpretation of the method, and to utilize it in reducing the time costs of frequency-domain broadband simulation. The interpretation here only uses knowledge of polynomials and linear algebra, hence it is straight forward and easy-to-understand. An efficient approach of frequency-domain broadband simulation is proposed as a sample application of the minimal rational interpolation. The approach gives rational function models of the concerned quantities with the lowest possible degrees. It is worth noting that although this manuscript focuses on fast broadband simulation, minimal rational interpolation is widely applicable. It could be used in scenarios like modeling tabulated frequency data of microwave circuits and interconnects, and broadband impedance matching. The proposed approach can be transplanted accordingly.

The outline of this paper is as follows. Section II presents our interpretation of the minimal rational interpolation. Section III gives a frequency-domain broadband simulation approach as a sample application of the minimal rational interpolation. Section IV shows the accuracy of the minimal rational interpolation by comparing it with vector fitting, and illustrates the efficiency of the proposed approach by two broadband simulation examples.

II. THE MINIMAL RATIONAL INTERPOLATION
Here we elaborate the minimal rational interpolation in an easy-to-understand way, and only use the knowledge of polynomials and linear algebra. Given data set

$$\{s_k, y_k\}, \quad k = 1, \dots, K, \tag{1}$$

where s_k represents the k-th Laplace frequency and equals $j2\pi f_k$, and y_k is the value of system variable at s_k. Rational interpolating problem wants to find

$$y(s) = n(s)/d(s) \tag{2}$$

that satisfies

$$y(s_k) = n(s_k)/d(s_k) = y_k, \text{ for } k = 1, \ldots, K. \tag{3}$$

$y(s)$ can be currents, fields, admittances, S-parameters, etc. Complexity of $y(s)$ is measured by the McMillan degree, which is defined as [26], [27].

$$\deg y(s) \triangleq \max\{\deg n(s), \deg d(s)\}. \tag{4}$$

For data set (1), $y(s)$ with different McMillan degrees exist. $y(s)$ will be non-unique unless it is required to be irreducible [28]. In view of numerical stability and physical realization, low-order models are always preferred. Hence, minimal rational interpolation looks for interpolating function with the minimal McMillan degree.

A. PREPARATION
In the following, we introduce an alternative solution of the minimal rational interpolation problem that finds the degree and coefficients of the rational function straightforwardly. In the beginning, we write the following two equations based on (3)

$$\bar{n}(s_k) - y_k \bar{d}(s_k) = 0, \text{ for } k = 1, \ldots, K, \tag{5}$$
$$\tilde{n}(s_k) - y_k \tilde{d}(s_k) = 0, \text{ for } k = 1, \ldots, K. \tag{6}$$

The second equation provides the freedom of constructing nonzero denominators, and this point will be explained in the next subsection. Denoting

$$\bar{n}(s) \triangleq \bar{n}_0 + \bar{n}_1 s + \bar{n}_2 s^2 + \cdots, \tag{7}$$
$$\bar{d}(s) \triangleq \bar{d}_0 + \bar{d}_1 s + \bar{d}_2 s^2 + \cdots, \tag{8}$$
$$\tilde{n}(s) \triangleq \tilde{n}_0 + \tilde{n}_1 s + \tilde{n}_2 s^2 + \cdots, \tag{9}$$
$$\tilde{d}(s) \triangleq \tilde{d}_0 + \tilde{d}_1 s + \tilde{d}_2 s^2 + \cdots, \tag{10}$$

we rewrite (5) and (6) as

$$
\begin{bmatrix}
1 & -y_1 & s_1 & -s_1 y_1 & s_1^2 & -s_1^2 y_1 & \cdots \\
1 & -y_2 & s_2 & -s_2 y_2 & s_2^2 & -s_2^2 y_2 & \cdots \\
\vdots & \vdots & \vdots & \vdots & \vdots & \vdots & \vdots \\
1 & -y_K & s_K & -s_K y_K & s_K^2 & -s_K^2 y_K & \cdots
\end{bmatrix}
\begin{bmatrix}
\bar{n}_0 & \tilde{n}_0 \\
\bar{d}_0 & \tilde{d}_0 \\
\bar{n}_1 & \tilde{n}_1 \\
\bar{d}_1 & \tilde{d}_1 \\
\bar{n}_2 & \tilde{n}_2 \\
\bar{d}_2 & \tilde{d}_2 \\
\vdots & \vdots
\end{bmatrix}
$$

$$
=
\begin{bmatrix}
0 & 0 \\
0 & 0 \\
0 & 0 \\
0 & 0 \\
0 & 0 \\
0 & 0 \\
\vdots & \vdots
\end{bmatrix} \tag{11}
$$

Since large numerical range might emerge in the above equation due to the powers of s, here we normalize f by

$$f' = 2(f - f_{\min})/(f_{\max} - f_{\min}) - 1, \tag{12}$$

such that the band $[f_{\min} \ f_{\max}]$ is mapped into $[-1 \ 1]$, which is around the center of the numerical range of computer.

Defining matrices F and G as

$$
F \triangleq
\begin{bmatrix}
s_1 & & & \\
& s_2 & & \\
& & \ddots & \\
& & & s_K
\end{bmatrix}, \quad
G \triangleq
\begin{bmatrix}
g_1 & g_2
\end{bmatrix}
$$

$$
=
\begin{bmatrix}
1 & -y_1 \\
1 & -y_2 \\
\vdots & \vdots \\
1 & -y_K
\end{bmatrix}, \tag{13}
$$

respectively, we abbreviate (11) as

$$
\begin{bmatrix}
F^0 g_1 & F^0 g_2 & F^1 g_1 & F^1 g_2 & F^2 g_1 & F^2 g_2 & \cdots
\end{bmatrix}
$$
$$
\cdot
\begin{bmatrix}
\tilde{n}_0 & \tilde{d}_0 & \tilde{n}_1 & \tilde{d}_1 & \tilde{n}_2 & \tilde{d}_2 & \cdots \\
\bar{n}_0 & \bar{d}_0 & \bar{n}_1 & \bar{d}_1 & \bar{n}_2 & \bar{d}_2 & \cdots
\end{bmatrix}^T
$$
$$
=
\begin{bmatrix}
0 & 0 & 0 & 0 & 0 & 0 & \cdots \\
0 & 0 & 0 & 0 & 0 & 0 & \cdots
\end{bmatrix}^T, \tag{14}
$$

where F^i is the i-th power of F of dimension $K \times K$, $F^i g_1$ and $F^i g_2$ are column vectors of dimension $K \times 1$. According to Cayley–Hamilton theorem and related results in Appendix A, $F^0 G, F^1 G, F^2 G, \cdots$ can be written as linear combinations of $F^0 G, F^1 G, \cdots, F^{K-1} G$. Hence, (14) is equivalent to

$$
\begin{bmatrix}
F^0 g_1 & F^0 g_2 & F^1 g_1 & F^1 g_2 & \cdots & F^{K-1} g_1 & F^{K-1} g_2
\end{bmatrix}
$$
$$
\cdot
\begin{bmatrix}
\tilde{n}_0 & \tilde{d}_0 & \tilde{n}_1 & \tilde{d}_1 & \cdots & \tilde{n}_{K-1} & \tilde{d}_{K-1} \\
\bar{n}_0 & \bar{d}_0 & \bar{n}_1 & \bar{d}_1 & \cdots & \bar{n}_{K-1} & \bar{d}_{K-1}
\end{bmatrix}^T
$$
$$
=
\begin{bmatrix}
0 & 0 & 0 & 0 & \cdots & 0 & 0 \\
0 & 0 & 0 & 0 & \cdots & 0 & 0
\end{bmatrix}^T. \tag{15}
$$

The above equation is of dimension $K \times 2K$, and there are $2K$ unknowns. Intuitively, the unknowns can be found by appropriate method, and hence $\bar{n}(s)$, $\bar{d}(s)$, $\tilde{n}(s)$, and $\tilde{d}(s)$ will be all of degree $K - 1$. In this sense, Cayley–Hamilton theorem provides natural bound on the orders of the four polynomials. However, two points should be noted here. The first point is that for K data points, rational interpolating function with the numerator and denominator both of order $K-1$ is not always necessary. Thus the orders of $\bar{n}(s)$, $\bar{d}(s)$, $\tilde{n}(s)$, and $\tilde{d}(s)$ could be lower than $K-1$. The second point is that (5) and (6) are not necessarily equivalent to (3). Before moving $\bar{d}(s)$ or $\tilde{d}(s)$ to the denominator position of (3), we should make sure that they are nonzero for all the abscissas $s_1, \ldots, s_K$, or else $\bar{n}(s_k)/\bar{d}(s_k)$ and $\tilde{n}(s_k)/\tilde{d}(s_k)$ will be undefined. In the next subsection, method to find the coefficients in the polynomials is given, and both the above two points are considered.

$$\begin{bmatrix} F^0 g_1 & F^0 g_2 & F^1 g_1 & F^1 g_2 & F^2 g_1 & F^2 g_2 & F^3 g_1 & F^3 g_2 & F^4 g_1 & F^4 g_2 \end{bmatrix}$$
$$\begin{matrix} \times & \times & \times & \times & \text{o} & \times & * & \text{o} & * & * \end{matrix}$$

FIGURE 1. Exemplary structure of (16), $K = 5$. 'x' indicates the independent vectors, 'o' indicates the primary dependent vector, and '∗' corresponds to the non-primary dependent vectors. The positions of the marks are by no means fixed as shown, and they depend on actual data.

B. CONSTRUCTING THE MINIMAL INTERPOLANT

In (15), $\begin{bmatrix} \bar{n}_0 & \bar{d}_0 & \bar{n}_1 & \bar{d}_1 & \cdots & \bar{n}_{K-1} & \bar{d}_{K-1} \end{bmatrix}^T$ and $\begin{bmatrix} \tilde{n}_0 & \tilde{d}_0 & \tilde{n}_1 & \tilde{d}_1 & \cdots & \tilde{n}_{K-1} & \tilde{d}_{K-1} \end{bmatrix}^T$ represent the coefficients of linear dependent relationships in

$$\begin{bmatrix} F^0 g_1 & F^0 g_2 & F^1 g_1 & F^1 g_2 & \cdots & F^{K-1} g_1 & F^{K-1} g_2 \end{bmatrix}. \quad (16)$$

Therefore, we will look for such relationships in the above matrix. To this end, we search the columns of the matrix in order from left to right, and stop the procedure once the obtained dependent relationships suffice for constituting the interpolating function. It is true that we can rearrange (15) and (16) in different forms. For example, putting the g_1 terms together and the g_2 terms together, we will have

$$\begin{bmatrix} F^0 g_1 & \cdots & F^{K-1} g_1 & F^0 g_2 & \cdots & F^{K-1} g_2 \end{bmatrix}$$
$$\cdot \begin{bmatrix} \tilde{n}_0 & \tilde{n}_1 & \cdots & \tilde{n}_{K-1} & \tilde{d}_0 & \tilde{d}_1 & \cdots & \tilde{d}_{K-1} \\ \bar{n}_0 & \bar{n}_1 & \cdots & \bar{n}_{K-1} & \bar{d}_0 & \bar{d}_1 & \cdots & \bar{d}_{K-1} \end{bmatrix}^T$$
$$= \begin{bmatrix} 0 & 0 & \cdots & 0 & 0 & 0 & \cdots & 0 \\ 0 & 0 & \cdots & 0 & 0 & 0 & \cdots & 0 \end{bmatrix}^T. \quad (17)$$

However, since column vectors of the first matrix in the above are searched in order from left to right, the resulting coefficients may have forms like $\begin{bmatrix} \bar{n}_0 & \bar{n}_1 & \cdots & \bar{n}_{K-1} & \bar{d}_0 \end{bmatrix}$. Consequently, the degree of the numerator is much larger than that of the denominator. On the contrary, (15) and (16) will make the difference between the degrees of the numerator and denominator small. It is commonly regarded that in Padé approximation, rational functions with the difference between the degrees of numerator and denominator less than one have the best fitting capability [7], [20]. As a result, searching (16) leads to rational interpolating function with lower McMillan degree.

Now we elaborate on how to find and exploit the dependent relationships in (16). For convenience, we use Fig. 1 to help explanation. In the beginning, we select $F^0 g_1$ as the first independent vector and mark it with '×'. Since the elements of g_2 are not the same unless y does not change over frequency, $F^0 g_2$ is independent of $F^0 g_1$, and we mark it with '×'. Next, we go to subsequent columns and continue the search. If a vector, for example, $F^{\kappa_1} g_j$, first becomes linearly dependent on its previous vectors, then we call it the first primary dependent vector, and mark it with 'o'. By the algorithm in Appendix B, we get the coefficients of the linear combination of dependent column. Substituting these coefficients (some of them may be zeros) into (7) and (8), we get $\bar{n}(s)$ and $\bar{d}(s)$ with the highest degree κ_1. For example, in Fig. 1, $\kappa_1 = 2$, $j = 1$, thus the first dependent relationship is

$$\bar{n}_0 F^0 g_1 + \bar{d}_0 F^0 g_2 + \bar{n}_1 F^1 g_1 + \bar{d}_1 F^1 g_2 + \bar{n}_2 F^2 g_1 = 0, \quad (18)$$

or explicitly,

$$\bar{n}_0 \begin{bmatrix} 1 \\ 1 \\ \vdots \\ 1 \end{bmatrix} + \bar{d}_0 \begin{bmatrix} -y_1 \\ -y_2 \\ \vdots \\ -y_K \end{bmatrix} + \bar{n}_1 \begin{bmatrix} s_1 \\ s_2 \\ \vdots \\ s_K \end{bmatrix} + \bar{d}_1 \begin{bmatrix} -s_1 y_1 \\ -s_2 y_2 \\ \vdots \\ -s_K y_K \end{bmatrix}$$
$$+ \bar{n}_2 \begin{bmatrix} s_1^2 \\ s_2^2 \\ \vdots \\ s_K^2 \end{bmatrix} = \begin{bmatrix} 0 \\ 0 \\ \vdots \\ 0 \end{bmatrix}. \quad (19)$$

The above is saying that

$$\bar{n}_0 + \bar{n}_1 s_k + \bar{n}_2 s_k^2 = (\bar{d}_0 + \bar{d}_1 s_k) y_k, \text{ for } k = 1, \ldots, K. \quad (20)$$

Hence, we have

$$\bar{n}(s) = \bar{n}_0 + \bar{n}_1 s + \bar{n}_2 s^2, \quad (21)$$
$$\bar{d}(s) = \bar{d}_0 + \bar{d}_1 s. \quad (22)$$

At this point, we check whether $\bar{d}(s)$ is nonzero for all $s_1, \ldots, s_K$. If so, we stop the search and take $\bar{d}(s)$ as the denominator, obtaining

$$y(s) = \bar{n}(s) / \bar{d}(s) \quad (23)$$

with $\deg y(s) = \kappa_1$, where κ_1 is the minimal McMillan degree.

On the other hand, if $\bar{d}(s)$ equals zero for some s_k, we can not take $\bar{d}(s)$ as the denominator. In such case we have to continue the search in order to find the second dependent relationship that will help constitute nonzero denominator. A fact that will be used later is that the vectors $F^i g_j$, where $i > \kappa_1$ and j is the same as that in $F^{\kappa_1} g_j$, also depend on their previous vectors. For example, in Fig. 1 we have $\kappa_1 = 2$, $j = 1$. Left multiplying (18) by F, we get

$$\bar{n}_0 F^1 g_1 + \bar{d}_0 F^1 g_2 + \bar{n}_1 F^2 g_1 + \bar{d}_1 F^2 g_2 + \bar{n}_2 F^3 g_1 = 0, \quad (24)$$

which indicates the dependence of $F^3 g_1$ (that is $i = 3$, $j = 1$). Proceeding similarly, we can also show the dependence of $F^4 g_1$. We call $F^3 g_1$ and $F^4 g_1$ the non-primary dependent vectors, and mark them by '∗'. In addition, one can find that the dependent relationship in (24) is the same as that in (18). Taking the first line element of (24), we have

$$s_1 (\bar{d}_0 + \bar{d}_1 s_1) y_1 = \bar{n}_0 s_1 + \bar{n}_1 s_1^2 + \bar{n}_2 s_1^3. \quad (25)$$

Thus, when $\bar{d}_0 + \bar{d}_1 s_1$ equals zero in (22), the left hand side of the above will also be zero, which means that the non-primary dependent vectors contain no valid information for constituting nonzero denominator.

Next, we claim that $F^{\kappa_2} g_{j'}$, where $\kappa_2 = K - \kappa_1$ and $j' \neq j$, must be dependent by using the facts that 1) matrix (16) has column rank K; 2) all the vectors before $F^{\kappa_1} g_j$ are independent; 3) vectors $F^i g_j$ with $i > \kappa_1$ are dependent. For example, in Fig. 1 the matrix has column rank 5, so the first four vectors are independent, and the fifth vector is the first primary dependent vector. Then, $F^2 g_2$ must be independent. Otherwise, using the same method as we deduce the dependence of $F^3 g_1$ and $F^4 g_1$, we will get that $F^3 g_2$ and $F^4 g_2$

are dependent. Then, the matrix will only have column rank four, and this contradicts the fact that the matrix has column rank five. As a result, $F^2 g_2$ must be independent. By now we have obtained all the five independent vectors, so $F^3 g_2$ must be dependent. Hence, $\kappa_2 = 3$, and $j' = 2$. $F^{\kappa_2} g_{j'}$ is called the second primary dependent vector. Since it appears after $F^{\kappa_1} g_j$, relationship $\kappa_1 \leq \kappa_2 \leq K - 1$ will always hold.

Substituting the coefficients of the second primary dependent relationship (some of them may be zeros) into (9) and (10), we get $\tilde{n}(s)$ and $\tilde{d}(s)$ with the highest degree κ_2. Let us assume the second primary dependent relationship in Fig. 1 as

$$\tilde{n}_0 F^0 g_1 + \tilde{d}_0 F^0 g_2 + \tilde{n}_1 F^1 g_1 + \tilde{d}_1 F^1 g_2 + \tilde{d}_2 F^2 g_2 + \tilde{d}_3 F^3 g_2 = 0. \tag{26}$$

Following a procedure similar to that between (18) and (22), we get

$$\tilde{n}(s) = \tilde{n}_0 + \tilde{n}_1 s, \tag{27}$$
$$\tilde{d}(s) = \tilde{d}_0 + \tilde{d}_1 s + \tilde{d}_2 s^2 + \tilde{d}_3 s^3. \tag{28}$$

In Appendix C, we prove that $\tilde{d}(s_k)$ and the previously obtained $\bar{d}(s_k)$ cannot be zero simultaneously for any k. Now the motivation for having $\tilde{n}(s)$ and $\tilde{d}(s)$ (or equivalently, having (6)) becomes clear: it provides the opportunity for constructing nonzero denominator when $\bar{d}(s)$ equals zero for some s_k. In this case, denominator of the rational interpolating function can be constructed as linear combination of $\bar{d}(s)$ and $\tilde{d}(s)$, i.e.,

$$p(s)\bar{d}(s) + \tilde{d}(s), \tag{29}$$

where $p(s)$ is any polynomial satisfying the constraint

$$p(s_k)\bar{d}(s_k) + \tilde{d}(s_k) \neq 0, \text{ for } k = 1, \ldots, K. \tag{30}$$

For keeping low complexity, it is preferable to set

$$\deg p(s) \leq \kappa_2 - \kappa_1. \tag{31}$$

Then, $\bar{n}(s)$ and $\tilde{n}(s)$ must follow the same linear combination as (29) to meet the interpolation requirements. Consequently, the rational function is of the form

$$y(s) = \frac{p(s)\bar{n}(s) + \tilde{n}(s)}{p(s)\bar{d}(s) + \tilde{d}(s)} \tag{32}$$

with $\deg y(s) = \kappa_2$, where κ_2 is the minimal McMillan degree.

At this point, we have found the solution to the minimal rational interpolation problem. For clarity, we summarize the main steps as follows:

1) Scale f according to (12), and compute matrix (16);
2) Search the columns of (16) in order from left to right, and find the first dependent vector $F^{\kappa_1} g_j$. Then, substitute the coefficients of the dependent relationship into (7) and (8), and get $\bar{n}(s)$ and $\bar{d}(s)$;
3) Check whether $\bar{d}(s)$ is nonzero for all $s_1, \ldots, s_K$. If so, (23) is the desired interpolating function with degree κ_1. Otherwise, go to the next step;

4) Set κ_2 to be $K - \kappa_1$, and select $F^{\kappa_2} g_{j'}$ ($j' \neq j$) as the second primary dependent vector. Find the coefficients in the dependent relationship and substitute them into (9) and (10), and get $\tilde{n}(s)$ and $\tilde{d}(s)$;
5) Choose any $p(s)$ satisfying $\deg p(s) \leq \kappa_2 - \kappa_1$ and (30), then (32) will be the solution with degree κ_2.

From the above steps, we see that with this method one does not need to estimate the complexity of the rational interpolating function, and can always get functions with the minimal McMillan degree. Owing to these properties, the method can be implemented as fully automatic program, and it is well suited as the interpolating algorithm in broadband simulation.

C. REMARKS ON PHYSICAL CONSISTENCY AND NUMERICAL STABILITY

By now we have finished the introduction of minimal interpolation as a mathematical method. In this sense, the method is general. However, when it is applied to fit realistic physical quantities and the resulting model is to be used together with other systems, physical consistency should be considered. Specifically, the model must be causal, stable, and passive [29], [30]. For linear time-invariant systems passivity implies causality [31]. As a result, only stability and passivity need to be satisfied. Since no attention was paid on physical consistency in the previous derivations, the resulting rational models have unstable poles and violate passivity constraint. In addition, the coefficients in the numerator and denominator polynomials are complex, and this leads to unrealizable model.

To solve the problem of complex coefficients and unstable poles, we suggest utilizing the method in [32]. Firstly, the real parts of the frequency response are fitted with even rational functions of squared variables by using the minimal rational interpolation. Then, poles of the even functions are found and those in the left half-plane are taken as the poles of the original rational functions. In the end, the coefficients in the numerator polynomials of the original functions are solved. At this point, the resulting rational functions will be stable and real-coefficient.

Passivity assurance has been studied extensively in macro-modelling [33]–[37]. It consists of two steps, namely, passivity check and passivity enforcement. As in vector fitting, the two steps are usually carried out as post processing of rational modeling. There are public domain codes for passivity assurance (for example, the RPdriver of the matrix fitting toolbox [36], [37]). The results of minimal rational interpolation, after being made stable and real-coefficient, can be processed by such routines so as to meet physical consistency constraints.

From the explicit form of (11), we know that the entries along each row of (16) are powers of frequency values. Therefore the computational procedure will be limited by the numerical range and precision of the computer. The normalization in (12) makes the procedure no longer limited by the numerical range. However, when the frequency range is wide

and the data change rapidly, high-order approximation should be used. At this time the procedure will still be limited by the numerical precision, as parts of the normalized frequencies are small and their high order powers are difficult to be represented. In such cases we suggest dividing the frequency range into sub-bands and fitting the data in each band individually. The cost is that one can no longer get a single rational model for the whole data.

III. APPLICATION IN BROADBAND SIMULATION

Nowadays, many full-wave numerical techniques are available for accurate analysis of EM systems. In these techniques quantities on all the mesh girds are taken as unknowns. As the complexity of the modeled objects increases, the number of unknowns also increases, leading to higher requirements on memory space and computing time. However, in many cases designers are only interested in part of the quantities within a frequency range. This motivates the idea of approximating the variations of quantities by rational interpolating functions, so the overall computational costs can be saved. Many works have been published on this topic [2], [11], [12], [15], [16], [19], [38]. Particularly, vector fitting is combined with AFS and PEEC method for extracting macromodel of interconnects [14]. In this section we give an efficient broadband simulation approach as a sample application of the previously introduced minimal rational interpolation. Like [14], the approach here also combines rational interpolation and AFS. The central idea is to fit the frequency-domain simulation results by rational interpolating functions, which are then checked and improved recursively by new simulation results. The aim is to achieve accurate and broadband results with reasonable computational costs. A flow diagram of the approach is shown in Fig. 2, and the main steps proceed as follows:

1) To begin, the start and end points of the frequency range are selected as initial frequency samples. Frequency-domain EM simulations are carried out at the two points, resulting in currents, fields, etc. Then quantities of concern are selected and put into a data set that will be fitted later. The specific choice of quantities depends on actual scenarios. For example, if the broadband admittances of a circuit are considered, then only the current coefficients at the circuit ports are selected. This choice will reduce the workload of interpolation.

2) Then, the quantities of interests are fitted individually by the minimal interpolation, obtaining rational functions with the lowest degrees. These functions are believed to be accurate at the data points. Depending on the attributes of the fitted data, the stability and passivity processing in Section II-C may be required for keeping physical consistency.

3) To assess the validity of the obtained interpolating functions, test frequency points are selected according to predefined rules, and EM simulations are performed at these points. In this work, test points are set to the intermediate values of interpolating input frequencies.
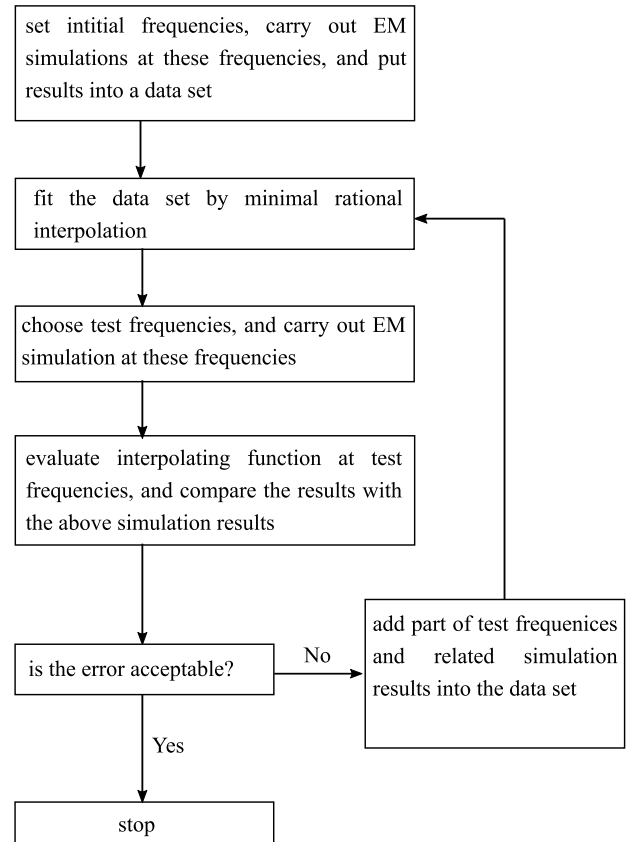

FIGURE 2. Flow diagram of the broadband simulation which exploits adaptive frequency sample and minimal rational interpolation.

4) The interpolating functions are evaluated at the test points, and the function values are compared with the above simulation results. To get a scalar number that indicates the validity of interpolating functions, we define the maximum relative error (MRE) as

$$MRE = \max_{j=1,...,J} \{ \max_{k=1,...,K} \{ |y_j(s_k) - y_{j,k}|/|y_{j,k}| \} \}, \quad (33)$$

where J denotes the number of fitted variables, K denotes the number of test frequencies, $y_{j,k}$ denotes the value of the j-th variable at the k-th test frequency, and $y_j(s_k)$ is value of the j-th interpolating function at the k-th test frequency. This definition gives the maximum relative error over all the test frequencies and all the fitted variables, hence it directly indicates the validity of interpolating functions. On occasion, $y_{j,k}$ is small or close to zero, and this makes the error definition in (33) invalid. In such case, the maximum root-mean-square (RMS) error can be used, which is defined as

$$MRMSE = \max_{j=1,...,J} \left\{ \sqrt{\frac{1}{K} \sum_{k=1}^{K} |y_j(s_k) - y_{j,k}|^2} \right\}. \quad (34)$$

5) If the error is larger than a prescribed criterion, it means that the current rational function models need to be improved by supplementing new contents to the interpolating data set. Since adding all the test frequencies into the data set will

make the degrees of interpolating functions growth rapidly, only the test frequencies with the first m maximum errors are added. Then the procedure goes to step 2.

6) Steps 2-5 are repeated until the error is less than the predefined threshold. Depending on the desired accuracy, the threshold can be adjusted. At this time, the variations of the quantities are captured by the rational functions, and the procedure is terminated. The resulting rational functions are then evaluated at desired frequencies.

The above steps follow an iterative procedure of 'fit data – check validity – add new data – fit data – · · · '. The approach has the following properties: Firstly, interpolating functions are generated automatically, and one does not need to interact with the program. This is due to the automatic property of the minimal rational interpolation. Secondly, the obtained rational functions always have low degrees due to the minimal property of the rational interpolation. Consequently, model order reduction is not required, and this is preferable for applications like physical realization. Thirdly, the approach is more efficient than the simple point-by-point simulation in terms of time costs. When the process is terminated, one just has to evaluate the rational functions at desired frequencies. Finally, like the other interpolation based method, the approach here does not solve for or storage derivations, so it costs less computational time and memory compared to the AWE based methods.

It should be stressed that the approach here is by no means ideal. It is just a sample application of the minimal rational interpolation in broadband computational electromagnetics. When the procedure stops, it just means that convergence is achieved under the predefined rules. Even if most of the frequency range is oversampled by the approach, some important features can still be missed due to local undersampling. Usually, some prior knowledge is needed to evaluate the validity of the rational models. The flow diagram in Fig. 2 is general. The fitting method, error definition, and the method of selecting test frequencies can be replaced, for example, by those in [14]. Several frequencies of the band can also be designated as the key points, where tests must be carried out. These measures will help to ensure that all the dynamics within the frequency range are captured by the final rational functions. As mentioned in Step 2), the stability and passivity processing in Section II-C may be required to make the rational functions physical consistent, but the actual choice depends on the scenarios. For example, scattering simulations of objects in frequency domain do not require stability and passivity. Finally, the approach fits the quantities of concern individually, hence the computational costs scale linearly with the number of quantities of interests. Further work is needed to study the possibility of fitting multiple quantities with rational functions sharing the same common poles and zeros, thus reducing the computational costs.

IV. EXAMPLES
In this section, we give two examples to demonstrate the effectiveness of minimal rational interpolation and the

practical value of the broadband simulation approach. Objects in the two examples are all PEC, and they are simulated by integral equation methods. The program is executed on a computer with Intel i7-3820QM CPU (8 cores at 2.7 GHz) and 32 GB RAM.

A. EXAMPLE 1: INTERCONNECTS
In this example, broadband admittances of the interconnects in Fig. 3 are considered. The structure is cut out of a realistic package board [39], [40], and the associated mesh has 3691 triangular patches and 5222 inner edges. The highest frequency supported by the mesh is about 40 GHz. There are four ports in the structure, and they are marked out by the arrows in the figure. First, we show the accuracy of minimal rational interpolation by fitting the Y_{31} parameter between 1 MHz - 40 GHz. There are 161 frequencies in all. The interval between the first and second frequencies is 0.249 GHz, and the intervals between the remaining frequencies are 0.25 GHz. Since the average size of the mesh is much smaller than the smallest wavelength of the frequency band, common MOM solver can not be used. Instead, an augmented electric field integral equation solver (A-EFIE), which is immune to low-frequency breakdown [39], [40], is adopted. Then the minimal rational interpolation is applied to fit the simulation results. The program finds a rational function with McMillan degree 22, and the function is compared with the original 161 data in Fig. 4. Fig. 4a and 4c illustrate that the function fits the original data quite well, and one can hardly distinguish them from the overlapped lines. Fig. 4b shows that the average value of the relative errors of the magnitudes is on the order of 1E-5. In theory, the error should equal zero at the
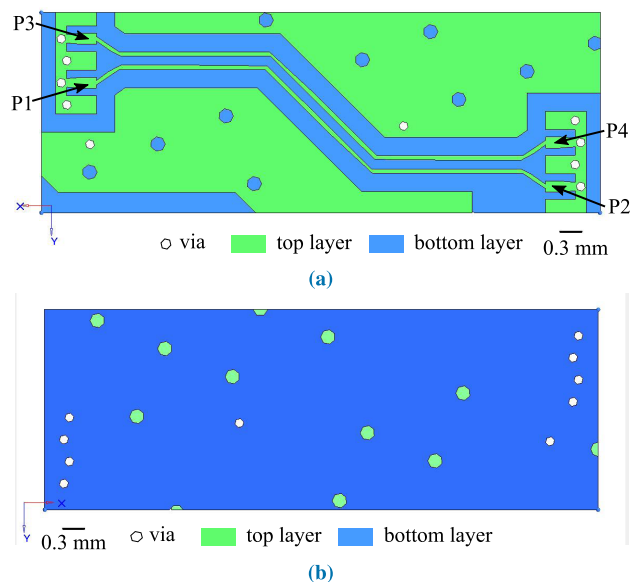

FIGURE 3. Geometry of the interconnects with (a) top layer upwards and (b) bottom layer upwards. The distance between the top layer and the bottom layer is 0.29 mm, and the two layers are connected by 7 vias. The over all dimension in the X-Y plane is 7.57 × 2.73 mm². P1, P2, P3, and P4 are exciting ports.

original data points. However, there are numerical errors in the program, so one can not get ideal fitting. It should be noted that stability and passivity enforcement is not implemented in our current program, so the result is accurate only in mathematical meaning.

For comparison, the commonly used vector fitting [13], [41], [42] is applied to fit the same data. Since the degree of rational model (or equivalently, the number of poles) is a necessary input parameter of the vector fitting program, it is specified as 8, 22, and 36, respectively. The degree of 22 is the same as that found by the minimal rational interpolation, while the degree of 36 is larger than the later. Passivity enforcement is turned off in the program. Results under the three degrees are also shown in Fig. 4. When the degree is 8, the relative errors of the magnitudes are on the order of 1, being very large and unacceptable. This demonstrates the necessity of providing appropriate order estimate in vector fitting. When the degree is underestimated inaccurate results will be obtained. On the contrary, the minimal rational interpolation finds the underlying degrees automatically, and the user is not required to provide the estimate. This facilitates its application in fully-automatic broadband simulation. The errors of vector fitting decrease as the input degrees increases to 22 and 36. However, the errors in the range of 5.25-14.25 and 21.75-34.75 GHz are still much larger than those of minimal rational interpolation. In particular, the errors at 10.25 GHz reach 0.56, while the error of minimal rational interpolation is less than 1E-6. This comparative example demonstrates the clear advantage of minimum interpolation in automatically producing high precision fittings with low order functions. In addition to accuracy, computational time is also a concern when embedding interpolating algorithms in fast frequency sweep. In the above example the minimal rational interpolation costs 0.29 second, and the vector fitting costs 0.13 second in each of the three fitting tasks. As the A-EFIE program uses about 44 seconds in simulating a single frequency point, the time taken by the two interpolating algorithms is negligible.

We then apply the proposed simulation approach to compute Y_{ij}, where $j = 1, \ldots, 4$ and $i \geq j$, between 1 GHz - 40 GHz. The approach calls A-EFIE solver to get tabulated data of the ten admittances, and interpolates them individually. The maximum number of newly added interpolation frequencies in each step is set to 12. The stopping criteria for the MRE is set to 3E-3. After seven steps of 'fit data – check validity – add new data', the error becomes 2E-3 and the process is terminated. The solid line in Fig. 5 shows the errors in the process. Fig. 6 shows the frequencies used by each step. In the figure, frequencies marked by 'o' are used to construct interpolation functions, while those marked by 'x' are used to check errors, and they are the intermediate of the 'o' points. There are a total of 81 frequency points, of which 41 (the 'o' points in the top line) are used to construct the final interpolation functions. Table 1 lists the complexities of the final ten rational functions, and the maximum degree is 20. To show the accuracies of these ten rational functions,
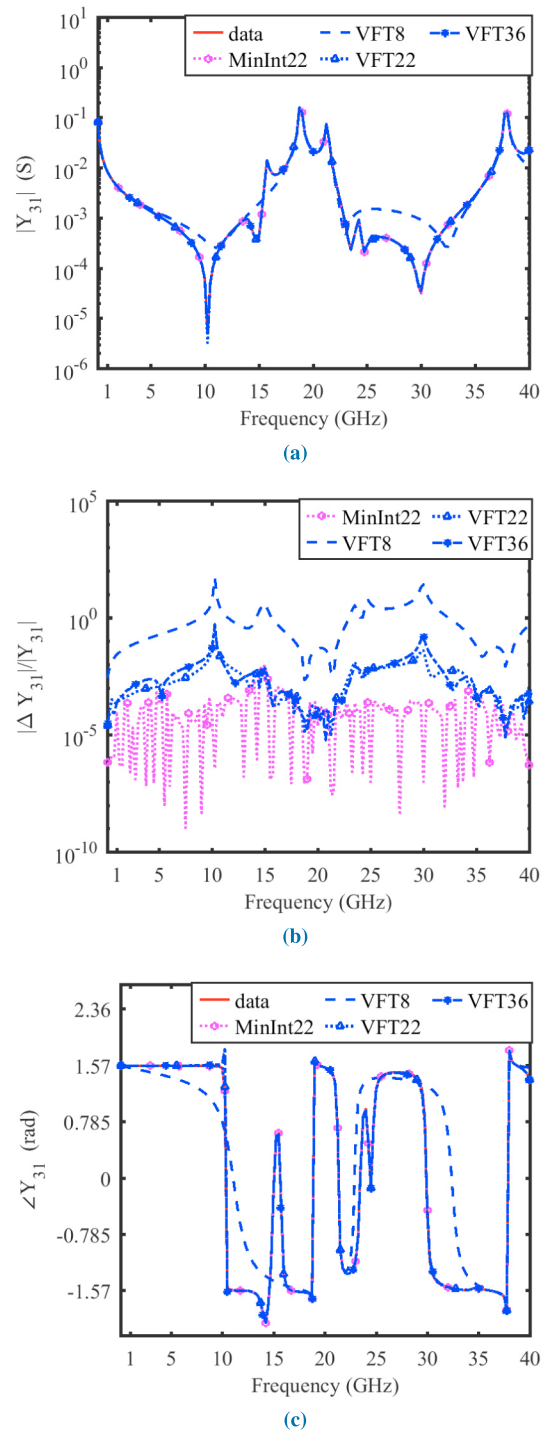
FIGURE 4. Comparison of the various interpolating functions with the original Y_{31} data. Legends in the figures are abbreviated for compactness. data: Original data; MinInt22: minimal rational interpolation with degree 22; VFT8: vector fitting with degree 8; VFT22: vector fitting with degree 22; VFT36: vector fitting with degree 36. (a) Magnitudes of the admittances. (b) Relative errors of the magnitudes. (c) Phases of the admittances.

we perform another simulation of the interconnects. This time the frequency step is set to 0.125 GHz, and the 313 frequencies are simulated one by one. This method is called 'point-by-point' simulation. The ten rational functions are evaluated at the same 313 frequencies and the obtained values
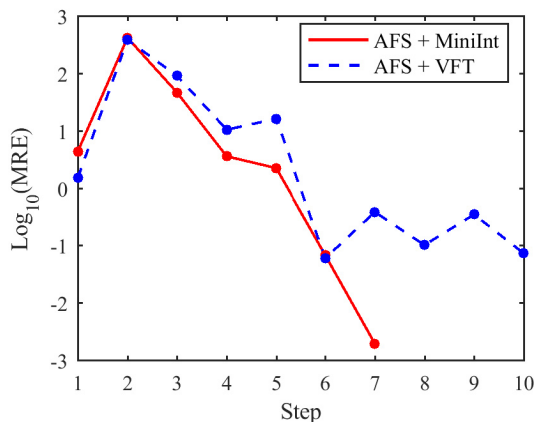
FIGURE 5. The maximum relative errors within each step of the broadband simulation of the interconnects.
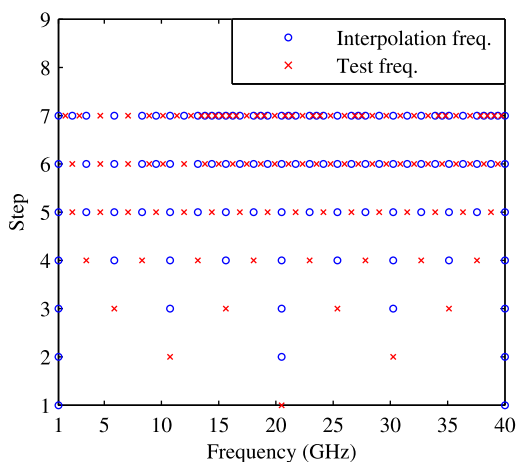

FIGURE 6. Frequencies used by each step of the broadband simulation of the interconnects.

TABLE 1. Degrees of the rational models of the admittances.

Method	Y_{11}	Y_{21}	Y_{31}	Y_{41}	Y_{22}
AFS + MiniInt	19	20	18	20	20
AFS + VFT[*]	40	40	40	40	40

Method	Y_{32}	Y_{42}	Y_{33}	Y_{43}	Y_{44}
AFS + MiniInt	19	19	21	20	20
AFS + VFT[*]	40	40	40	40	40

[*] The results correspond to the 7-th step of the iteration.

**TABLE 2.** Costs for computing broadband admittances of the interconnects.

Method	Freq. number	Time (hours)	Memory (MB)
point-by-point, step 0.25 GHz	157	1.65	4434.8[*]
point-by-point, step 0.125 GHz	313	3.38	4434.8
AFS + MiniInt	81	0.89	4440.7
AFS + VFT	81	1	4439.3

[*] Note that for A-EFIE, the number of unknown is 5222+3691-1=8192. LU decomposition is applied to solve the matrix equation. For details, see [40].

are found to agree with the point-by-point simulation results. For illustration, Fig. 7 plots the comparison of Y_{42}. Note that the sharp peaks in the curves are captured exactly by the rational function models. Table 2 lists the simulation costs of the proposed approach and the point-by-point method for getting the broadband admittances. Obviously, the proposed approach is more time-efficient than the later, and uses negligible additional memory.

As mentioned in section III, the broadband simulation approach is general, and the fitting process therein can be implemented by other methods. For reference and comparison, we re-run the above example using the vector fitting as a substitute for the minimal rational interpolation, while keeping all other parameters unchanged. For vector fitting the degrees of rational functions are necessary input parameters. In order to ensure the accuracy of fitting, we set the degrees as one less than the lengths of the data to be fitted. As the simulation goes on, the lengths of data increase and the degrees are updated accordingly. The errors in the simulation process are plotted as the dashed line in Fig. 5, whose convergence rate is slower than that of minimal rational interpolation. The errors at the 7 and 10-th steps are 0.39 and 0.08, respectively.

Up to the 7-th step of the iteration, 81 frequencies are simulated and 41 of them are used to construct the interpolating functions. The degrees of these functions are all 40, being twice of the degrees of those functions generated by minimal rational interpolation. The accuracies of these rational models are also verified by comparing with the data of point-by-point simulation with dense frequency sampling. As a representative example, the case of Y_{42} is drawn as the dashed lines with triangle labels in Fig. 7. The relative errors of magnitudes show the model exhibit comparable accuracies as that generated by AFS in combination with minimal rational interpolation in the band of 10-40 GHz. However, in the band of 1-9.6 GHz the model exhibit lower accuracies than the latter. Seven of the other nine models exhibit similar behavior. To sum up the above comparison, the advantage of applying the minimum interpolation algorithm in adaptive broadband simulation lies in using low-order functions to achieve high-precision rational models, thus accelerating the simulation speed.
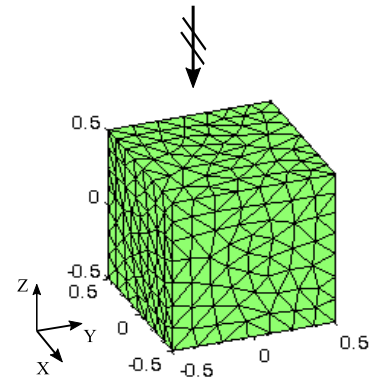
B. EXAMPLE 2: CUBE UNDER PLANE WAVE ILLUMINATION

In this example, the approach is applied to simulate the scattering of a cube between 2-22 GHz. The cube is shown

(a)

(b)

(c)
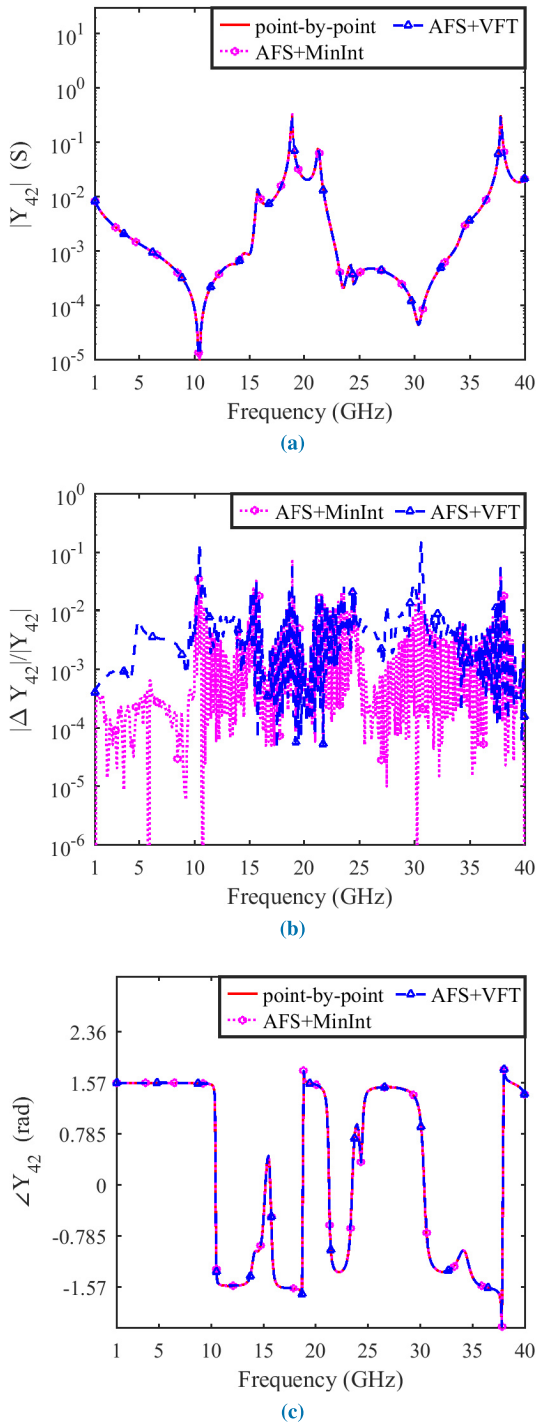
FIGURE 7. Y_{42} **obtained by point-by-point simulation, broadband approach that combines AFS with minimal rational interpolation, and combines AFS with vector fitting. (a) Magnitudes. (b) Relative errors of the magnitudes. (c) Phases.**

in Fig. 8 and its side length is 1 cm. The incident plane wave propagates along the $-z$ direction, and the electric field is in the $+x$ direction. The EM solver called by the approach is MOM, and there are a total of 975 Rao-Wilton-Glisson (RWG) basis functions [43]. Coefficients of the basis

FIGURE 8. A cube under plane wave illumination. Unit: 1 cm. The mesh consists of 650 triangular patches and 975 inner edges.
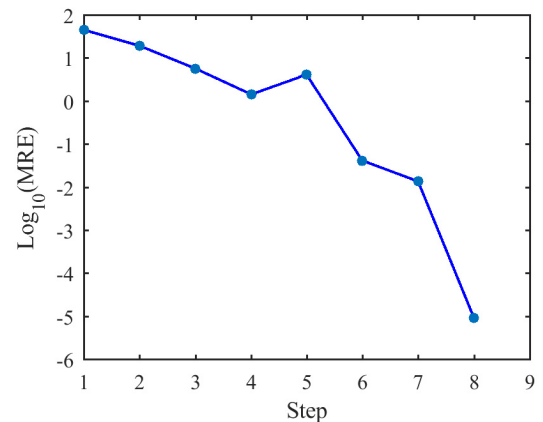
FIGURE 9. The maximum relative errors within each step of the broadband simulation of the cube.

functions are chosen as the quantities to be fitted since they are closely related to the near fields and change rapidly over frequency. This choice should be more challenging than interpolating the far fields. The maximum number of newly added interpolation frequencies in each step is set to 8. The stopping threshold on the maximum relative error is set to 1E-3. In the eighth step of the iteration, the error becomes 9.5E-6 and the process is terminated. Fig. 9 shows the maximum relative error within each step. Fig. 10 plots the frequencies used by each step. There are 81 frequency points in all, 41 of which are used for interpolation (marked by 'o') and the other 40 are used for assessing errors (marked by '×'). The maximum McMillan degree of the 975 rational functions is 15, and the minimal is 13.

To check the accuracies of the rational function models of the currents, we rerun the MOM code in point-by-point manner with step of 0.1 GHz, and the current coefficients at all the frequencies are written to files. Then values of the rational functions are computed at the same frequencies and compared with the written data. The differences in Fig. 11 show that the relative magnitude errors are less than 1E-5 and the absolute phase errors are less than 1.5E-5 rad. This demonstrate the accuracies of rational models, so the fields
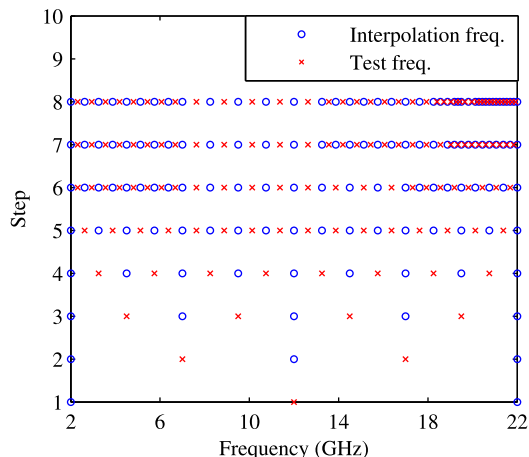
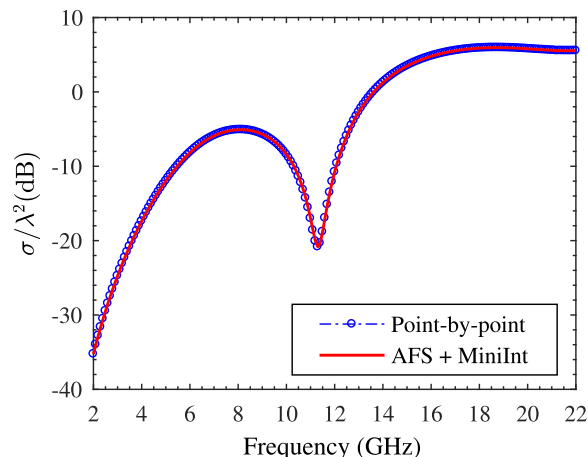**FIGURE 10.** Frequencies used by each step of the broadband simulation of the cube.
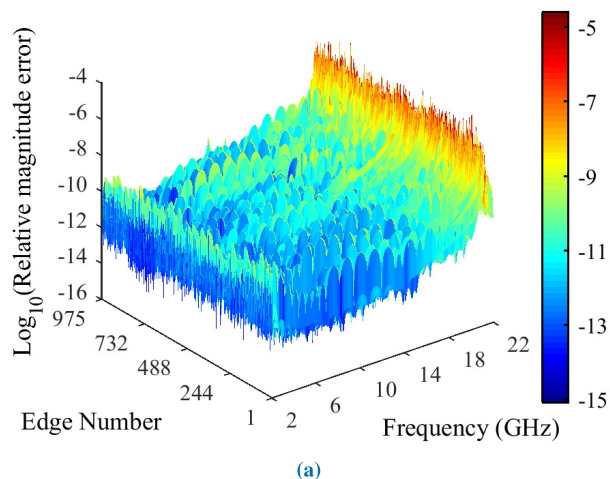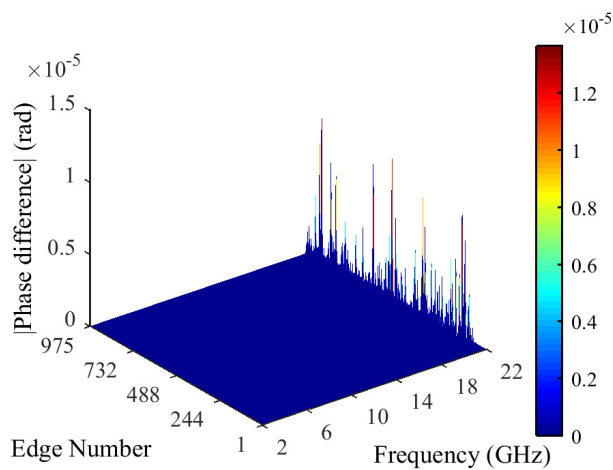

(a)

(b)

FIGURE 11. Differences between rational function models of current coefficients on the cube and the results of point-by-point simulation. (a) Relative magnitude differences. (b) Absolute values of the phase differences.

can be computed faithfully. Fig. 12 compares the backward RCS derived from the rational models with that obtained by point-by-point simulation. The two curves overlap and

FIGURE 12. Backward RCS of the cube in the z direction.

TABLE 3. Costs for computing the induced currents on the cube.

Method	Freq. number	Time (seconds)	Memory (MB)
point-by-point, step 0.1 GHz	201	302	91.8
AFS + MiniInt	81	125	123.3

cannot be distinguished. Table 3 lists the costs of the two approaches for simulating the cube. It can be seen that the proposed approach uses much less time than the point-by-point simulation while consuming comparable memory. This superiority will be even more pronounced as the problem size increases. Therefore, the proposed approach is quite effective in accelerating frequency-domain broadband simulation, and can help to save time in related study.

V. CONCLUSION

This work introduces the minimal rational interpolation from point view of linear algebra, and makes the algorithm easy to understand. In addition, this work also presents an efficient broadband simulation approach that exploits the minimal rational interpolation and adaptive frequency sampling. The approach is fully automatic and always gives rational function models with the minimal McMillan degrees. Examples illustrate the power and efficiency of the approach. Future improvements of this work include optimizing the strategies of adaptive frequency sampling, possibly by utilizing machine learning, such the final rational models generated by the approach will not miss any details in the interested frequency band. Although this work focuses on the application in fast broadband simulation, minimal rational interpolation is widely applicable. Possible scenarios include modeling experimental and simulation data and broadband impedance matching. With physical consistency enforcement as postprocessing, it could also be applied in macromodel extraction.

In these scenarios the proposed approach can be transplanted accordingly.

APPENDIXES
APPENDIX A
CAYLEY–HAMILTON THEOREM AND RELATED RESULTS

Cayley–Hamilton Theorem says that every square matrix satisfies its characteristic equation. Specifically, let A be a matrix of dimension $n \times n$, and let

$$p(\lambda) = \det(A - \lambda I) = \alpha_0 + \alpha_1 \lambda + \cdots + \alpha_n \lambda^n \quad (35)$$

be its characteristic polynomial. Then,

$$p(A) = \alpha_0 I + \alpha_1 A + \cdots + \alpha_n A^n = 0. \quad (36)$$

For proof of the theorem, see Chapter 2 of [44].

Let $f(\lambda)$ be any polynomial in λ, then there are unique polynomials $g(\lambda)$ and $r(\lambda)$ such that

$$f(\lambda) = p(\lambda)g(\lambda) + r(\lambda), \quad (37)$$

where $\deg r(\lambda) \leq n - 1$. Assuming

$$r(\lambda) = \beta_0 + \beta_1 \lambda + \cdots + \beta_{n-1} \lambda^{n-1}, \quad (38)$$

and exploiting $p(A) = 0$, we have $f(A) = r(A)$, which means that any polynomials of A can be expressed as

$$f(A) = \beta_0 I + \beta_1 A + \cdots + \beta_{n-1} A^{n-1}. \quad (39)$$

The above equation implies that A^m, where $m \geq n$, can be written as linear combination of $I, A, A^2, \ldots, A^{n-1}$.

APPENDIX B
SEARCH LINEAR DEPENDENT COLUMNS
WITHIN A MATRIX

In Section II-B, it is required to search the linear dependent columns of a matrix in order from left to right. The method we use is column-searching, which is a parallel implementation of the row-searching algorithm in page 550-551 of [44]. Here we elaborate the method by a simple example. Assuming A is a 4×5 matrix, we first transform it into reduced row echelon form by using routines like Gauss Jordan elimination with partial pivoting, and get

$$\bar{A} = \begin{bmatrix} 1 & 0 & 0 & \bar{a}_{14} & 0 \\ 0 & 1 & 0 & \bar{a}_{24} & 0 \\ 0 & 0 & 1 & \bar{a}_{34} & 0 \\ 0 & 0 & 0 & 0 & 1 \end{bmatrix}. \quad (40)$$

The above expression means that the fourth column of A can be represented as linear combination of the first three columns, namely,

$$A(:, 4) = \bar{a}_{14} A(:, 1) + \bar{a}_{24} A(:, 2) + \bar{a}_{34} A(:, 3). \quad (41)$$

As a result, we get the dependent relationship and coefficients in the linear combination.

Note that the matrix in this example is general and no assumption is made on its form. Eqn. (16) brings special property to the positions of dependent columns. Refer to Section II-B for the discussion.

APPENDIX C
PROOF OF THE FACT THAT $\bar{D}(S)$ and $\tilde{D}(S)$ CANNOT BE ZERO AT THE SAME INTERPOLATION FREQUENCY

Let us assume the first primary dependent relationship of (16) as

$$\bar{n}_0 F^0 g_1 + \bar{d}_0 F^0 g_2 + \cdots + \bar{d}_{\kappa_1 - 1} F^{\kappa_1 - 1} g_2 + \bar{n}_{\kappa_1} F^{\kappa_1} g_1 = 0, \quad (42)$$

then it follows that $j = 1$ and $j' = 2$. Using a procedure similar to the one between (18) and (22), we have

$$\bar{n}(s) = \bar{n}_0 + \bar{n}_1 s + \cdots + \bar{n}_{\kappa_1} s^{\kappa_1}, \quad (43)$$
$$\bar{d}(s) = \bar{d}_0 + \bar{d}_1 s + \cdots + \bar{d}_{\kappa_1 - 1} s^{\kappa_1 - 1}, \quad (44)$$

which satisfy

$$\bar{n}(s_k) - y_k \bar{d}(s_k) = 0, \text{ for } k = 1, \ldots, K. \quad (45)$$

If $\bar{d}(s)$ equals zero for some s_k, e.g., s_1, then the above implies that $\bar{n}(s)$ and $\bar{d}(s)$ share the common polynomial factor $s - s_1$. We cancel the factor in the above three equations, and get

$$\bar{n}'_0 + \bar{n}'_1 s_k + \cdots + \bar{n}'_{\kappa_1 - 1} s_k^{\kappa_1 - 1} - y_k(\bar{d}'_0 + \bar{d}'_1 s_k + \cdots$$
$$+ \bar{d}'_{\kappa_1 - 2} s_k^{\kappa_1 - 2}) = \begin{cases} \alpha, & k = 1 \\ 0, & k = 2, \ldots, K, \end{cases} \quad (46)$$

where α is some nonzero constant. If α equals zero, then the left hand side of the above equals zero for all $k = 1, \ldots, K$, implying that $F^{\kappa_1 - 1} g_1$ is dependent. Apparently, this is in conflict with the assumption that $F^{\kappa_1} g_1$ is the first dependent vector. Consequently, α must be nonzero.

Assuming the second primary dependent relationship in (16) as

$$\tilde{n}_0 F^0 g_1 + \tilde{d}_0 F^0 g_2 + \cdots + \tilde{n}_{\kappa_2} F^{\kappa_2} g_1 + \tilde{d}_{\kappa_2} F^{\kappa_2} g_2 = 0, \quad (47)$$

we have

$$\tilde{n}(s) = \tilde{n}_0 + \tilde{n}_1 s + \cdots + \tilde{n}_{\kappa_2} s^{\kappa_2}, \quad (48)$$
$$\tilde{d}(s) = \tilde{d}_0 + \tilde{d}_1 s + \cdots + \tilde{d}_{\kappa_2} s^{\kappa_2}, \quad (49)$$

which satisfy

$$\tilde{n}(s_k) - y_k \tilde{d}(s_k) = 0, \ k = 1, \ldots, K. \quad (50)$$

If $\tilde{d}(s)$ also equals zero at s_1, then we have

$$\tilde{n}'_0 + \tilde{n}'_1 s_k + \cdots + \tilde{n}'_{\kappa_2 - 1} s_k^{\kappa_2 - 1} - y_k(\tilde{d}'_0 + \tilde{d}'_1 s_k + \cdots$$
$$+ \tilde{d}'_{\kappa_2 - 1} s_k^{\kappa_2 - 1}) = \begin{cases} \beta, & k = 1 \\ 0, & k = 2, \ldots, K, \end{cases} \quad (51)$$

where β is some nonzero constant.

Multiplying (46) by β and (51) by α, and then subtracting the results, we have

$$
\begin{aligned}
&(\beta \bar{n}_0' - \beta \bar{d}_0' y_k - \alpha \tilde{n}_0' + \alpha \tilde{d}_0' y_k) + (\beta \bar{n}_1' - \beta \bar{d}_1' y_k - \alpha \tilde{n}_1' \\
&\quad + \alpha \tilde{d}_1' y_k)s_k + \cdots + (-\beta \bar{d}_{\kappa_1-2}' y_k)s^{\kappa_1-2} + \beta \bar{n}_{\kappa_1-1}' s_k^{\kappa_1-1} \\
&\quad - \alpha \tilde{n}_{\kappa_2-1}' s_k^{\kappa_2-1} + \alpha \tilde{d}_{\kappa_2-1}' y_k s_k^{\kappa_2-1} \\
&= \begin{cases} 0, & k = 1 \\ 0, & k = 2, \ldots, K. \end{cases}
\end{aligned} \tag{52}
$$

The above equation indicates that $F^{\kappa_2-1}g_2$ (corresponding to the last term in the left hand side of the above) is dependent. However, this is contradicts the fact that $F^{\kappa_2}g_2$ is the second primary dependent vector and all the vectors $F^i g_2$ with $i < \kappa_2$ should be independent. Therefore, $\bar{d}(s)$ and $\tilde{d}(s)$ cannot be zero at the same interpolation frequency.

REFERENCES

[1] E. K. Miller, "Model-based parameter estimation in electromagnetics: Part I. Background and theoretical development," *IEEE Antennas Propag. Mag.*, vol. 40, no. 2, pp. 42–52, Feb. 1998.

[2] E. K. Miller, "Model-based parameter estimation in electromagnetics: Part II. Applications to EM observables," *IEEE Antennas Propag. Mag.*, vol. 40, no. 2, pp. 51–65, Apr. 1998.

[3] E. K. Miller, "Model-based parameter estimation in electromagnetics: Part III. Applications to EM integral equations," *IEEE Antennas Propag. Mag.*, vol. 40, no. 3, pp. 49–66, Jun. 1998.

[4] Y. Wang, H. Ling, J. Song, and W. C. Chew, "A frequency extrapolation algorithm for FISC," *IEEE Trans. Antennas Propag.*, vol. 45, no. 12, pp. 1891–1893, Dec. 1997.

[5] S. Yan, S. Ren, Z. Nie, S. He, and J. Hu, "Efficient analysis of electromagnetic scattering from electrically large complex objects by using phase extracted basis functions," *IEEE Antennas Propag. Mag.*, vol. 54, no. 5, pp. 88–108, May 2012.

[6] L. T. Pillage and R. A. Rohrer, "Asymptotic waveform evaluation for timing analysis," *IEEE Trans. Comput.-Aided Design Integr. Circuits Syst.*, vol. 9, no. 4, pp. 352–366, Apr. 1990.

[7] C. J. Reddy, M. D. Deshpande, C. R. Cockrell, and F. B. Beck, "Fast RCS computation over a frequency band using method of moments in conjunction with asymptotic waveform evaluation technique," *IEEE Trans. Antennas Propag.*, vol. 46, no. 8, pp. 1229–1233, Aug. 1998.

[8] Z.-G. Qian and W. C. Chew, "Enhanced A-EFIE with perturbation method," *IEEE Trans. Antennas Propag.*, vol. 58, no. 10, pp. 3256–3264, Oct. 2010.

[9] J. P. Zhang and J. M. Jin, "Preliminary study of AWE method for FEM analysis of scattering problems," *Micro. Opt. Tech. Lett*, vol. 17, no. 1, pp. 7–12, Jan. 1998.

[10] J. W. Wu, Z. G. Qian, J. E. Schutt-Ainé, and W. C. Chew, "Fast solution of low-frequency complex problems over a frequency band using enhanced A-EFIE and FMM," *Micro. Opt. Tech. Lett*, vol. 56, no. 9, pp. 2153–2158, Sep. 2014.

[11] K. Kottapalli, T. K. Sarkar, Y. Hua, E. K. Miller, and G. J. Burke, "Accurate computation of wide-band response of electromagnetic systems utilizing narrow-band information," *IEEE Trans. Microw. Theory Techn.*, vol. 39, no. 4, pp. 682–687, Apr. 1991.

[12] R. S. Adve, T. K. Sarkar, S. M. Rao, E. K. Miller, and D. R. Pflug, "Application of the Cauchy method for extrapolating/interpolating narrowband system responses," *IEEE Trans. Microw. Theory Techn.*, vol. 45, no. 5, pp. 837–845, May 1997.

[13] B. Gustavsen and A. Semlyen, "Rational approximation of frequency domain responses by vector fitting," *IEEE Trans. Power Del.*, vol. 14, no. 3, pp. 1052–1061, Jul. 1999.

[14] G. Antonini, D. Deschrijver, and T. Dhaene, "Broadband rational macromodeling based on the adaptive frequency sampling algorithm and the partial element equivalent circuit method," *IEEE Trans. Electromagn. Compat.*, vol. 50, no. 1, pp. 128–137, Feb. 2008.

[15] R. Lehmensiek and P. Meyer, "Creating accurate multivariate rational interpolation models of microwave circuits by using efficient adaptive sampling to minimize the number of computational electromagnetic analyses," *IEEE Trans. Microw. Theory Techn.*, vol. 49, no. 8, pp. 1419–1430, Aug. 2001.

[16] Y. Ding, K.-L. Wu, and D. G. Fang, "A broad-band adaptive-frequency-sampling approach for microwave-circuit EM simulation exploiting Stoer-Bulirsch algorithm," *IEEE Trans. Microw. Theory Techn.*, vol. 51, no. 3, pp. 928–934, Mar. 2003.

[17] S. Lefteriu and A. C. Antoulas, "Modeling multi-port systems from frequency response via tangential interpolation," in *Proc. IEEE Workshop Signal Propag. Interconnects*, May 2009, pp. 1–4.

[18] S. Lefteriu and A. C. Antoulas, "A new approach to modeling multi-port systems from frequency-domain data," *IEEE Trans. Comput.-Aided Design Integr. Circuits Syst.*, vol. 29, no. 1, pp. 14–27, Jan. 2010.

[19] M. Kabir and R. Khzazka, "Loewner-matrix based efficient algorithm for frequency sweep of high-speed modules," in *Proc. IEEE 21st Conf. Elect. Perform. Electron. Packag. Syst.*, Oct. 2012, pp. 185–188.

[20] E. Chiprout and M. S. Nakhla, *Asymptotic Waveform Evaluation and Moment Matching for Interconnect Analysis*. Boston, MA, USA: Kluwer, 1994.

[21] A. E. Ruehli, "Equivalent circuit models for three-dimensional multi-conductor systems," *IEEE Trans. Microw. Theory Techn.*, vol. 22, no. 3, pp. 216–221, Mar. 1974.

[22] J. Stoer and R. Bulirsch, *Introduction to Numerical Analysis*. New York, NY, USA: Springer-Verlag, 1993.

[23] A. J. Mayo and A. C. Antoulas, "A framework for the solution of the generalized realization problem," *Linear Algebra Appl.*, vol. 425, nos. 2–3, pp. 634–662, Sep. 2007.

[24] Y. Wang, C. Lei, G. K. H. Pang, and N. Wong, "MFTI: Matrix-format tangential interpolation for modeling multi-port systems," in *Proc. Design Autom. Conf.*, Jun. 2010, pp. 683–686.

[25] A. C. Antoulas and B. D. Q. Anderson, "On the scalar rational interpolation problem," *IMA J. Math. Control Inf.*, vol. 3, nos. 2–3, pp. 61–88, 1986.

[26] A. C. Antoulas and J. C. Willems, "Minimal rational interpolation and prony's method," in *Analysis and Optimization of Systes* (Lecture Notes in Control and Information Sciences), vol. 144. Berlin, Germany: Springer, 1990, pp. 297–306.

[27] A. C. Antoulas, "On the solution of the minimal rational interpolation problem," *Linear Algebra Appl.*, vols. 137–138, pp. 511–573, Aug. 1990.

[28] N. Macon and D. E. Dupree, "Existence and uniqueness of interpolating rational functions," *Amer. Math. Monthly*, vol. 69, no. 8, pp. 751–759, Oct. 1962.

[29] W. Mai, J. Hu, P. Li, and H. Zhao, "An efficient and stable 2-D/3-D hybrid discontinuous Galerkin time-domain analysis with adaptive criterion for arbitrarily shaped antipads in dispersive parallel-plate pair," *IEEE Trans. Microw. Theory Techn.*, vol. 65, no. 10, pp. 3671–3681, Oct. 2017.

[30] W. Mai, P. Li, C. G. Li, M. Jiang, W. Hao, L. Jiang, and J. Hu, "A straightforward updating criterion for 2-D/3-D hybrid discontinuous Galerkin time-domain method controlling comparative error," *IEEE Trans. Microw. Theory Techn.*, vol. 66, no. 4, pp. 1713–1722, Apr. 2018.

[31] P. Triverio, S. Grivet-Talocia, M. S. Nakhla, F. G. Canavero, and R. Achar, "Stability, causality, and passivity in electrical interconnect models," *IEEE Trans. Adv. Packag.*, vol. 30, no. 4, pp. 795–808, Nov. 2007.

[32] W. T. Beyene and J. E. Schutt-Ainé, "Efficient transient simulation of high-speed interconnects characterized by sampled data," *IEEE Trans. Compon., Packag., Manuf. Technol. B*, vol. 21, no. 1, pp. 105–114, Feb. 1998.

[33] D. Saraswat, R. Achar, and M. Nakhla, "Passive macromodels of microwave subnetworks characterized by measured/simulated data," in *IEEE MTT-S Int. Microw. Symp. Dig.*, vol. 2, Jun. 2003, pp. 999–1002.

[34] S. Grivet-Talocia, "Passivity enforcement via perturbation of Hamiltonian matrices," *IEEE Trans. Circuits Syst. I, Reg. Papers*, vol. 51, no. 9, pp. 1755–1769, Sep. 2004.

[35] A. Lamecki and M. Mrozowski, "Equivalent SPICE circuits with guaranteed passivity from nonpassive models," *IEEE Trans. Microw. Theory Techn.*, vol. 55, no. 3, pp. 526–532, Mar. 2007.

[36] B. Gustavsen, "Fast passivity enforcement for pole-residue models by perturbation of residue matrix eigenvalues," *IEEE Trans. Power Del.*, vol. 23, no. 4, pp. 2278–2285, Oct. 2008.

[37] A. Semlyen and B. Gustavsen, "A half-size singularity test matrix for fast and reliable passivity assessment of rational models," *IEEE Trans. Power Del.*, vol. 24, no. 1, pp. 345–351, Jan. 2009.

[38] Y. Kim and H. Ling, "On the optimal sampling strategy for model-based parameter estimation using rational functions," *IEEE Trans. Antennas Propag.*, vol. 54, no. 2, pp. 762–765, Feb. 2006.

[39] Z. G. Qian and W. C. Chew, "An augmented electric field integral equation for high-speed interconnect analysis," *Microw. Opt. Technol. Lett.*, vol. 50, no. 10, pp. 2658–2662, Oct. 2008.

[40] Z.-G. Qian and W. C. Chew, "Fast full-wave surface integral equation solver for multiscale structure modeling," *IEEE Trans. Antennas Propag.*, vol. 57, no. 11, pp. 3594–3601, Nov. 2009.

[41] B. Gustavsen, "Improving the pole relocating properties of vector fitting," *IEEE Trans. Power Del.*, vol. 21, no. 3, pp. 1587–1592, Jul. 2006.

[42] D. Deschrijver, M. Mrozowski, T. Dhaene, and D. D. Zutter, "Macromodeling of multiport systems using a fast implementation of the vector fitting method," *IEEE Microw. Wireless Compon. Lett.*, vol. 18, no. 6, pp. 383–385, Jun. 2008.

[43] S. M. Rao, D. Wilton, and A. Glisson, "Electromagnetic scattering by surfaces of arbitrary shape," *IEEE Trans. Antennas Propag.*, vol. AP-30, no. 3, pp. 409–418, May 1982.

[44] C.-T. Chen, *Linear System Theory and Design*. New York, NY, USA: CBS College Publishing, 1984.
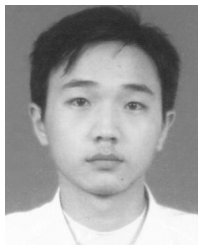
JUN WEI WU was born in Henan, China. He received the B.S. degree in electronic engineering from Shandong University, China, in 2008, and the Ph.D. degree in radio physics from Wuhan University, China, in 2015. From 2012 to 2014, he was a Visiting Scholar at the University of Illinois at Urbana–Champaign. He is currently holding a postdoctoral position at Southeast University, China. His research interests include computational electromagnetics, metamaterial design, and remote sensing.

TIE JUN CUI (M'98–SM'00–F'15) received the B.Sc., M.Sc., and Ph.D. degrees in electrical engineering from Xidian University, Xi'an, China, in 1987, 1990, and 1993, respectively.

In March 1993, he joined the Department of Electromagnetic Engineering, Xidian University, and became an Associate Professor, in November 1993. From 1995 to 1997, he was a Research Fellow at the Institut fur Hochstfrequenztechnik und Elektronik, University of Karlsruhe, Karlsruhe, Germany. In July 1997, he joined the Center for Computational Electromagnetics, Department of Electrical and Computer Engineering, University of Illinois at Urbana–Champaign, first as a Postdoctoral Research Associate, and then a Research Scientist. In September 2001, he became a Cheung-Kong Professor with the Department of Radio Engineering, Southeast University, Nanjing, China, where he is the Associate Dean of the School of Information Science and Engineering, and the Associate Director of the State Key Laboratory of Millimeter Waves. Since 2013, he has been a Representative of People's Congress of China. He is a Co-Editor of the book entitled *Metamaterials-Theory, Design, and Applications* (Springer, 2009) and the author of six book chapters. He has published more than 400 peer-reviewed journal articles in *Science*, PNAS, *Nature Communications*, *Physical Review Letters*, and many IEEE Transactions. His research interests include metamaterials, computational electromagnetic, wireless power transfer, and millimeter wave technologies, which have been cited by more than 13 500 times. He was elected as a Fellow of the Chinese Academy of Sciences, in 2019. He received a Research Fellowship from Alexander von Humboldt Foundation, Bonn, Germany, in 1995, and a Young Scientist Award from the International Union of Radio Science, in 1999. He was awarded a Cheung Kong Professor under Cheung Kong Scholar Program by the Ministry of Education, China, in 2001, the National Science Foundation of China for Distinguished Young Scholars, in 2002, the Special Government Allowance awarded by the Department of State, China, in 2008, the Award of Science and Technology Progress from Shaanxi Province Government, in 2009, was awarded by a May 1st Labour Medal by Jiangsu Province Government, in 2010, the First Prize of Natural Science from Ministry of Education, China, in 2011, and the Second Prize of National Natural Science, China, in 2014. His research works have been selected as one of the "10 Breakthroughs of China Science in 2010," "Best of 2010" in New Journal of Physics, Research Highlights in Europhysics News, Journal of Physics D: Applied Physics, Applied Physics Letters, and Nature China. His work has been reported by Nature News, Science, MIT Technology Review, Scientific American, and New Scientists. According to ELSEVIER, he is one of the Most Cited Chinese Researchers. He is an active reviewer for *Science*, *Nature Materials*, *Nature Photonics*, *Nature Physics*, *Nature Communications*, *Physical Review Letters*, *Advanced Materials*, and a series of IEEE Transactions. He was an Associate Editor of the IEEE Transactions on Geoscience and Remote Sensing and a Guest Editor in the *Science China Information Sciences*. He has served as an Editorial Staff in the *IEEE Antennas and Propagation Magazine*, and is in the editorial boards of Progress in Electromagnetic Research and the *Journal of Electromagnetic Waves and Applications*. He has served as the General Co-Chair of the International Workshops on Metamaterials, in 2008 and 2012, the TPC Co-Chair of Asian Pacific Microwave Conference, in 2005, and the Progress in Electromagnetic Research Symposium, in 2004.

• • •